

# Probing Velocity Dependent Self-Interacting Dark Matter with Neutrino Telescopes

Denis S. Robertson and Ivone F. M. Albuquerque

Instituto de Física,  
Universidade de São Paulo, Brazil

E-mail: [denistefanrs@gmail.com](mailto:denistefanrs@gmail.com), [ifreire@if.usp.br](mailto:ifreire@if.usp.br)

**Abstract.** Self-interacting dark matter models constitute an attractive solution to problems in structure formation on small scales. A simple realization of these models considers the dark force mediated by a light particle which can couple to the Standard Model through mixings with the photon or the  $Z$  boson. Within this scenario we investigate the sensitivity of the IceCube-DeepCore and PINGU neutrino telescopes to the associated muon neutrino flux produced by dark matter annihilations in the Sun. Despite the model's simplicity, several effects naturally appear: momentum suppressed capture by nuclei, velocity dependent dark matter self-capture, Sommerfeld enhanced annihilation, as well as the enhancement on the neutrino flux due to mediator late decays. Taking all these effects into account, we find that most of the model relevant parameter space can be tested by the three years of data already collected by the IceCube-DeepCore. We show that indirect detection through neutrinos can compete with the strong existing limits from direct detection experiments, specially in the case of isospin violation.

**Keywords:** Dark matter, Neutrinos, Particle physics, Neutrino Telescopes

**ArXiv ePrint:** [1234.56789](https://arxiv.org/abs/1234.56789)

---

## Contents

<b>1</b>	<b>Introduction</b>	<b>1</b>
<b>2</b>	<b>Velocity Dependent SIDM model</b>	<b>2</b>
2.1	Light Mediator Couplings to the SM	4
<b>3</b>	<b>Dark Matter Capture and Annihilation in the Sun</b>	<b>6</b>
<b>4</b>	<b>Neutrino Signal and Background</b>	<b>9</b>
<b>5</b>	<b>IceCube-DeepCore and PINGU Sensitivity to vdSIDM</b>	<b>12</b>
<b>6</b>	<b>Conclusions</b>	<b>13</b>

---

## 1 Introduction

Cosmological observations position  $\Lambda$ CDM as the standard model of cosmology. In this picture the Universe is dominated by dark energy (consistent with a cosmological constant  $\Lambda$ ) and collisionless cold dark matter (CDM). Despite its great success at large scales ( $\vartheta \gtrsim \text{Mpc}$ ), the CDM hypothesis encounters some potential difficulties describing smaller scales [1, 2]. These arise since observations do not agree with predictions from structure formation simulations. One of these problems is the core-cusp [3] discrepancy between the profiles of dark matter halos observed in dwarf and low surface brightness galaxies, which present a flat density core [4, 5] and the density profiles found in high resolution N-body CDM simulations, which steeply grow toward the center [6–8]. More recently the so called too big to fail (TBTF) problem [9, 10] came into evidence, and refers to the fact that  $\Lambda$ CDM simulations for Milky Way–like galaxies predict a number of massive subhalos that are too dense to be consistent with our observed galaxy’s dwarf satellites.

A promising possibility to solve or at least alleviate these problems is self-interacting dark matter (SIDM) [11]. Within this scenario dark matter particles interact with each other, allowing energy transfer from the external hotter regions of a dark matter halo to its cooler center. As a consequence the halo central density decreases forming a cored profile. Several SIDM simulations support this hypothesis, leading to a better agreement with observations when compared to CDM simulations [12–14]. To alleviate the TBTF problem, it is shown that the ratio between the dark matter self-interaction cross section and its mass must be within  $0.1 - 0.5 \lesssim \sigma/m_\chi \lesssim 10 - 50 \text{ cm}^2/\text{g}$  [15–17]. On the observational side there are very strong constraints on  $\sigma/m_\chi$ . Among these, the most stringent comes from analysis of the Bullet Cluster [18, 19] and other colliding clusters [20]. There are also more model dependent constraints as the ones from indirect dark matter probes through neutrino detection [21], and from simulations of structure formation [15–17], and based on dark matter halo shapes and density profiles of galaxies and clusters [22, 23]. All these combined require that  $0.1 \lesssim \sigma/m_\chi \lesssim 0.5 \text{ cm}^2/\text{g}$ , and thus exclude a large fraction of SIDM as a solution to the CDM small scale problems.

Nevertheless, these observations are reconciled if the dark matter self-interacting cross section depends on the particles’ relative velocity. These scenarios (vdSIDM), occur naturally

in SIDM models containing a dark force described by a Yukawa potential [24–26]. In these simple models the cross section is large at low velocities and falls rapidly as the relative velocity increases, so they alleviate the TBTF problem of dwarf satellites whose velocities are characteristically low (around  $\sim 10$  km/s). At the same time, vdSIDM also evades the strong constraints from larger astrophysical systems mentioned above (which have characteristic velocities between  $\sim 200 - 4000$  km/s).

In spite of its simplicity, vdSIDM models have a rich phenomenology. As an example, besides their non-trivial self-scattering cross section [26], their annihilation is enhanced by the Sommerfeld effect [27, 28]. When mixing between the dark force mediator and the Standard Model (SM) is considered, dark matter particles can scatter with nucleons, which in conjunction with the fact that their annihilation produces SM particles, opens up many possibilities for vdSIDM detection. Possible couplings are kinetic mixing with the photon or mass mixing through the  $Z$  or the Higgs boson. Several of these models have been probed, either by direct detection [29, 30] or indirect detection techniques [31, 32], imposing quite strong constraints on specific vdSIDM models.

In this work we explore how vdSIDM modifies the high energy neutrino flux from dark matter annihilation in the Sun, extending our work which indirectly constrains non velocity dependent SIDM [21]. We estimate the vdSIDM annihilation neutrino rate, and by comparing it to the atmospheric neutrino background IceCube-DeepCore’s and PINGU’s neutrino telescopes’ sensitivity to vdSIDM. We therefore provide grounds for an independent and complementary probe on vdSIDM.

Our analysis considers thermal symmetric dark matter models where self-interactions are mediated by a dark vector boson which couples to the SM via mass mixing with the  $Z$  boson and kinetic mixing. We consistently considered all the relevant phenomenology: dark matter self-interactions, enhanced annihilation due to the Sommerfeld effect, momentum suppression for dark matter–nucleon scatterings, and the possibility of enhanced neutrino signal due to the mediator late decays [33]. This latter effect was very recently studied focusing mainly on the possibility of new gamma ray and charged lepton signatures of dark matter coupled to the SM through dark photons [34] and collisionless dark matter [35]. Additionally, we considered a few combinations for the mixing parameters, leading to different dark matter couplings with neutrons and protons. We also compare our results with those from direct detection analysis.

We organize this paper as follows: section 2 briefly describes the vdSIDM model assumed in this analysis, and summarize current constraints on the model parameters. Section 3 describes how we estimate the dark matter capture and annihilation rates in the Sun. This is followed by our predictions for the signal and background events in section 4. The discussion of our results follows in section 5, and we conclude in the last section.

## 2 Velocity Dependent SIDM model

We consider the dark matter particle  $\chi$  as a Dirac fermion which couples to a vector mediator  $\phi_\mu$  of a dark  $U(1)_\chi$  gauge interaction through the Lagrangian term:

$$\mathcal{L} = g_\chi \bar{\chi} \gamma^\mu \chi \phi_\mu, \quad (2.1)$$

where  $g_\chi$  is the coupling constant. This interaction gives rise to dark matter self-scatterings and annihilations. We also take the dark matter as symmetric, with equal abundance of particles and anti-particles.

In the non-relativistic limit, dark matter self-interactions can be described by a Yukawa potential [24, 25, 36, 37]

$$V(r) = \pm \frac{\alpha_\chi}{r} e^{-m_\phi r}, \quad (2.2)$$

where  $\alpha_\chi = g_\chi^2/(4\pi)$  is the dark fine structure constant,  $m_\phi$  the mediator mass and  $r$  the relative distance between the dark matter particles. This potential is attractive ( $-$ ) for  $\chi\bar{\chi}$  scatterings, and repulsive ( $+$ ), for  $\chi\chi$  and  $\bar{\chi}\bar{\chi}$ .

The self-scattering cross section is determined [26] by numerically solving the Schrödinger equation with the Yukawa potential. A partial wave analysis is used when the classical (Born) limit breaks down at  $m_\chi v/m_\phi \lesssim 1$  ( $\alpha_\chi m_\chi/m_\phi \gtrsim 1$ ). Figure 1 shows the self-scattering transfer cross section <sup>1</sup>,  $\sigma_T = \int d\Omega (1 - \cos\theta) d\sigma_{\chi\chi}/d\Omega$ , as a function of the relative velocity, for both attractive (solid curves) and repulsive potentials (dashed curves). The strong dependence of the self-scattering cross section on the velocity is evident, decreasing several orders of magnitude as the velocity goes from  $v = 10$  to 1000 km/s. Also, for the attractive case, the velocity dependence is not trivial, presenting several resonances.

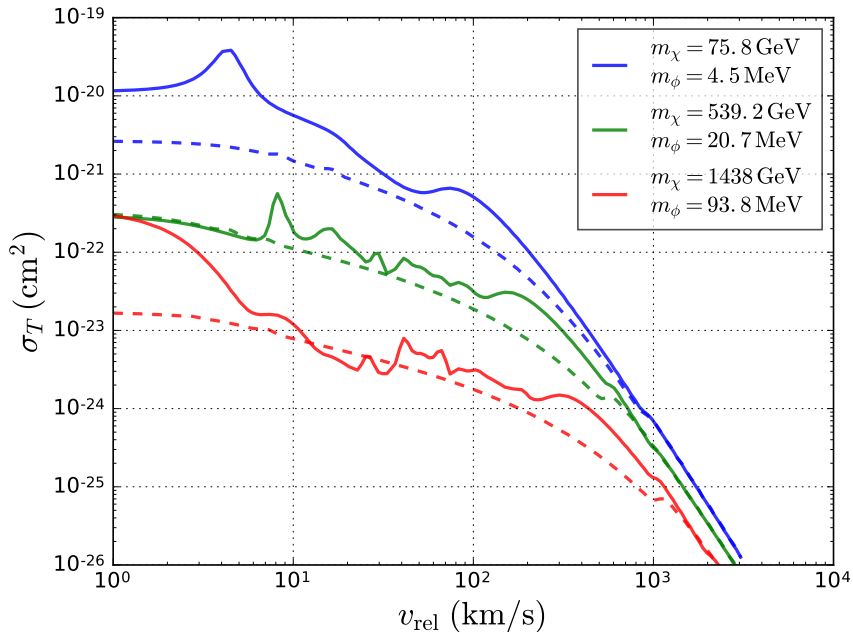


**Figure 1.** Self-scattering dark matter cross section as a function of the relative velocity. Attractive potential (solid curves) and repulsive potentials (dashed curves) are shown for different  $m_\chi$  and  $m_\phi$  values.

The dark matter annihilation cross section at tree level is given by

$$(\sigma_a v)^{\text{tree}} = \frac{\pi \alpha_\chi^2}{m_\chi^2} \sqrt{1 - \left(\frac{m_\phi}{m_\chi}\right)^2}. \quad (2.3)$$

<sup>1</sup>In common with the literature, we used  $\sigma_T$  as an effective cross section that relates the dark matter particle physics to the results from simulations of structure evolution. For details see [26].

However, for low relative velocities, it can greatly increase due to the Sommerfeld effect [38]. This is caused by the attractive self-interactions that distort the wave function of the incoming dark matter particles increasing their annihilation probability. The annihilation cross section can then be represented by

$$\sigma_a v = S(v) \times (\sigma_a v)^{\text{tree}}, \quad (2.4)$$

where the Sommerfeld factor  $S(v)$  can be computed numerically in an analogous way as for the self-scattering cross section [27, 39] or analytically by approximating the Yukawa potential by the Hulthen potential [28, 40, 41]. Using the latter, the Sommerfeld factor is given by

$$S = \frac{\pi}{a} \frac{\sinh(2\pi ac)}{\cosh(2\pi ac) - \cos(2\pi\sqrt{c - (ac)^2})}, \quad (2.5)$$

where  $a = v/(2\alpha_\chi)$  and  $c = 6\alpha_\chi m_\chi/(\pi^2 m_\phi)$ .

Additionally, we consider that the dark matter annihilation process  $\chi\bar{\chi} \rightarrow \phi\phi$  sets the dark matter relic density by thermal freeze-out. This requirement fixes the value of  $\alpha_\chi$  for given values of  $(m_\chi, m_\phi)$ . This relic density is determined taking the Sommerfeld enhancement into consideration [26, 28]. This effect turns out important only for heavy dark matter  $m_\chi \gtrsim 1$  TeV.

## 2.1 Light Mediator Couplings to the SM

We assume that the dark sector couples to the SM via the  $\phi$  mediator, which allows production of known particles from dark matter annihilation in the Sun. Following a phenomenological approach, we consider that the  $\phi$  mediator mixes with the photon  $\gamma$  and the  $Z$  boson through

$$\mathcal{L}_{\text{mixing}} = \frac{\varepsilon_\gamma}{2} \phi_{\mu\nu} F^{\mu\nu} + \varepsilon_Z m_Z^2 \phi_\mu Z^\mu, \quad (2.6)$$

where  $\phi_{\mu\nu} \equiv \partial_\mu \phi_\nu - \partial_\nu \phi_\mu$  and  $F^{\mu\nu}$  are, respectively, the mediator and the photon field strengths. The first term corresponds to the photon kinetic mixing while the second one to the mass mixing with the  $Z^2$ . We take the limit of very small mixing parameters  $\varepsilon_\gamma, \varepsilon_Z \ll 1$ . Both terms are relevant in our analysis, since the  $Z$  mixing allows the production of high energy neutrinos through  $\phi$  decays, and the kinetic mixing the dark matter scattering off protons, which contributes significantly to its capture in the Sun. Both mixings have been widely studied within the context of vector portal dark matter, dark photon and dark  $Z$  searches [27, 32, 42–49] and also for vdSIDM direct detection [29].

If only kinetic mixing is present, the  $\phi$  decays predominantly into  $e^+e^-$ , with decay rate

$$\Gamma_\phi^\gamma = \frac{\alpha_{\text{em}} m_\phi \varepsilon_\gamma^2}{3}. \quad (2.7)$$

In the case of  $Z$  mixing, the total decay rate is given by

$$\Gamma_\phi^Z = \frac{\alpha_{\text{em}} m_\phi \varepsilon_Z^2 (1 - \sin^2 \theta_W + 2 \sin^4 \theta_W)}{6 \sin^2 \theta_W \cos^2 \theta_W}. \quad (2.8)$$

---

<sup>2</sup>Although the latter term explicitly breaks gauge invariance, it can arise in extensions of the SM through the insertion of additional Higgs and dark Higgs, as in Ref.[42]. In our work, we do not go into the details of the dark matter particle physics models, but take a phenomenological approach considering both mixing parameters  $\varepsilon_\gamma, \varepsilon_Z$  independently.

where the neutrino channel dominates with a branching ratio  $BR_{(\phi \rightarrow \nu \bar{\nu})} \approx 6/7$ , leaving a  $BR_{(\phi \rightarrow e^+ e^-)} \approx 1/7$  for the  $e^+ e^-$  channel. Therefore, for given values of  $\varepsilon_\gamma$  and  $\varepsilon_Z$ , the total decay rate is  $\Gamma_\phi = \Gamma_\phi^\gamma + \Gamma_\phi^Z$  and the branching ratio to neutrinos  $BR_{(\phi \rightarrow \nu \bar{\nu})} = \Gamma_{(\phi \rightarrow \nu \bar{\nu})}^Z / \Gamma_\phi$ .

An additional consequence of the mediator mixing with SM particles is the DM scattering with nucleons via  $\phi$  exchange, which are crucial for dark matter capture in the Sun. This interaction is represented by

$$\mathcal{L}_{\text{int}} = e\phi_\mu(\varepsilon_p \bar{p} \gamma^\mu p + \varepsilon_n \bar{n} \gamma^\mu n), \quad (2.9)$$

where  $\varepsilon_p, \varepsilon_n$  are the effective coupling to protons and neutrons, and parameterized [29] respectively by:

$$\varepsilon_p = \varepsilon_\gamma + \frac{\varepsilon_Z}{4 \sin \theta_W \cos \theta_W} (1 - 4 \sin^2 \theta_W) \approx \varepsilon_\gamma + 0.05 \varepsilon_Z \quad (2.10)$$

$$\varepsilon_n = -\frac{\varepsilon_Z}{4 \sin \theta_W \cos \theta_W} \approx -0.6 \varepsilon_Z. \quad (2.11)$$

Thus, in the case of kinetic mixing, the mediator couples only to the charged proton. For  $Z$  mixing, the mediator couples mainly to neutrons. So, for these models isospin violation, i.e. different interactions strengths to protons and neutrons, arises naturally.

The spin-independent dark matter scattering with a nucleus  $N$ , carrying atomic number  $Z$  and mass number  $A$ , and in the zero momentum transfer limit ( $q^2 = 0$ ) is given by

$$\sigma_{\chi N}^{\text{SI}} = \frac{16\pi \alpha_{\text{em}} \alpha_\chi \mu_{\chi N}^2}{m_\phi^4} (\varepsilon_p Z + \varepsilon_n (A - Z))^2, \quad (2.12)$$

where  $\mu_{\chi N}$  is the dark matter–nucleus reduced mass. However, the mediator masses we are exploring are comparable to the transferred momentum in the DM scatterings with the Sun’s nuclei, which are typically of the order of  $q \sim 10$  MeV. Therefore, the cross section is momentum dependent and cannot be approximated by a contact interaction [29, 50, 51]. We take this into account by considering a suppression factor

$$\sigma_{\chi N}^{\text{SI}}(q^2) = \sigma_{\chi N}^{\text{SI}}(q^2 = 0) \times \frac{m_\phi^4}{(m_\phi^2 + q^2)^2}, \quad (2.13)$$

where the momentum transfer is given by  $q = \sqrt{2m_N E_R}$  and  $E_R \simeq \mu_{\chi N}^2 v^2 / m_N$  is the typical nuclear recoil energy.

Before describing the dark matter accumulation in the Sun and its associated signal we briefly summarize some relevant constraints on the parameters we just described.

In order not to violate the standard Big Bang nucleosynthesis, a lower bound on the mixing parameters  $\varepsilon_\gamma, \varepsilon_Z \gtrsim 10^{-10} \times \sqrt{10 \text{ MeV} / m_\phi}$  comes from the requirement that the  $\phi$  mediator decays fast enough, with a lifetime  $\tau_\phi \lesssim 1$  s [52]. Also, analysis of supernovae cooling through mediator emission establish strong constraints on the kinetic mixing parameter, excluding  $\varepsilon_\gamma \sim 10^{-10} - 10^{-7}$  for  $m_\phi \sim 1 - 100$  MeV [53–56]. Recent works have revised these analysis including the plasma effects of finite temperature and density [57, 58] and specifically [58] excludes  $\varepsilon_\gamma \gtrsim 10^{-8}$  for  $m_\phi \sim 10 - 40$  MeV and  $\varepsilon_\gamma \gtrsim 10^{-9}$  for  $m_\phi \sim 10$  MeV independently of the details in their modeling.

Other constraints come from beam dump and fixed target experiments such as SLAC E137 [45, 59], the LSND neutrino experiment [60, 61] and CHARM [62, 63]. Among these,

the strongest results correspond to E137, excluding  $\varepsilon_\gamma \gtrsim 10^{-7}$  for mediator masses  $m_\phi \lesssim 400$  MeV.

Additional constraints come from dark matter direct detection searches. Recent analysis have used the results from XENON100, LUX and SuperCDMS experiments to constrain vdSIDM models [29, 30]. Their results indicate that most of the relevant parameter space with  $m_\chi \gtrsim 10$  GeV if  $\varepsilon_\gamma, \varepsilon_Z = 10^{-8}$  is excluded, and  $m_\chi \gtrsim 30$  GeV if  $\varepsilon_\gamma, \varepsilon_Z = 10^{-9}$ .

Finally, there are also strong constraints from indirect detection searches. Recent analysis that included the enhancement in dark matter annihilations due to the Sommerfeld effect [31, 32] have found that the observations of gamma rays by Fermi-LAT [64], the positron and anti-proton flux by AMS-02 [65–67] and particularly the CMB by Planck [68] exclude a large part of the parameter space of vdSIDM that can alleviate the CDM small scale problems. However, models with  $m_\phi \lesssim 1$  MeV still remain a possible solution in the case of  $\phi - Z$  mass mixing.

In our analysis we focus on vdSIDM models with mixing parameters between  $\varepsilon_\gamma, \varepsilon_Z \sim 10^{-10} - 10^{-8}$  and with  $m_\chi \sim 1$  GeV - TeV and  $m_\phi \sim 1 - 100$  MeV.

### 3 Dark Matter Capture and Annihilation in the Sun

In this section we analyze how dark matter self-scattering affects the capture and annihilation processes in the Sun. The time evolution for the total number of dark matter particles and anti-particles<sup>3</sup> in the Sun  $N_\chi$  is

$$\dot{N}_\chi = \Gamma_c + \Gamma_s - 2\Gamma_a, \quad (3.1)$$

where  $\Gamma_a$  is the dark matter annihilation rate,  $\Gamma_c$  its capture rate due to scatterings with the Sun’s nuclei, and  $\Gamma_s$  its self-capture rate. Note that evaporation processes were neglected, given that they are negligible for DM masses  $m_\chi \geq 4$  GeV [69, 70]. Neither the effects of dark matter bound states formation are considered, since these are expected to be negligible for most of the parameter space that we study [32, 71]<sup>4</sup>.

The DM capture rate due to scatterings with the Sun’s nuclei is given by

$$\Gamma_c = 4.8 \times 10^{24} \text{ s}^{-1} \frac{\rho_\chi}{0.3 \text{ GeV/cm}^3} \left( \frac{270 \text{ km/s}}{\bar{v}} \right) \left( \frac{\text{GeV}}{m_\chi} \right) \sum_i \mathcal{F}(m_\chi, N_i) \left( \frac{\sigma_{\chi N_i}}{10^{-40} \text{ cm}^2} \right), \quad (3.2)$$

where we take the local dark matter halo density  $\rho_\chi = 0.4 \text{ GeV/cm}^3$  [72, 73], and its velocity dispersion  $\bar{v} = 270 \text{ km/s}$ . The sum is over all nuclear species  $N_i$  in the Sun and the factor  $\mathcal{F}(m_\chi, N_i)$  denotes the product of several factors for each nuclear element. It includes their mass fraction, distribution in the Sun, and the kinematic and form factor suppressions [74]. For the first two of these factors, we took updated values from [75] and [76]. The dark matter–nucleus cross section  $\sigma_{\chi N_i}$  is given by equation (2.13).

The dark matter capture rate has been determined in [77–79], and extended in [80, 81] to include self-interactions. The SIDM high energy neutrino rate in IceCube has been determined in [21]. Here we extend these procedures to account for the velocity dependence

<sup>3</sup>From here on when we mention dark matter particles, we consider them in conjunction with their anti-particles, unless specified.

<sup>4</sup>The formation and decay of dark matter bound states in the Sun can contribute positively to dark matter indirect signals for large dark matter masses ( $m_\chi \gtrsim 2$  TeV) [32], making our results for neutrino telescopes’ sensitivities conservative at these  $m_\chi$  values.

of the self-scattering cross section  $\sigma_{\chi\chi}(v_{\text{rel}})$ , and also the spatial and velocity distributions of the dark matter particles in the Sun. The self-capture rate can be written as  $\Gamma_s = C_s N_\chi$ , where  $N_\chi$  is the number of captured dark matter particles and

$$C_s = \int \frac{f_{\text{halo}}^{\text{DM}}(u)}{u} \sigma^{\text{eff}}(v_{\text{rel}}) f_{\text{sun}}^{\text{DM}}(r, u') (v^2 - u'^2 - u^2) \Theta(v^2 - u'^2 - u^2) 4\pi r^2 dr d\theta du' du, \quad (3.3)$$

where

$$f_{\text{halo}}^{\text{DM}}(u) = \sqrt{\frac{6}{\pi}} \left( \frac{\rho_\chi}{m_\chi} \right) \frac{1}{\tilde{v}} e^{-\frac{3}{2}(u/\tilde{v})^2} e^{-\frac{3}{2}(\tilde{v}/\tilde{v})^2} u^2 \sinh\left(\frac{3u\tilde{v}}{\tilde{v}^2}\right) \frac{1}{u\tilde{v}} \quad (3.4)$$

is the dark matter velocity distribution in the halo,  $\tilde{v} = 220$  km/s is the Sun's velocity and  $v$  is the escape velocity at a distance  $r$  from the center of the Sun. We assume that the dark matter particles are thermally distributed in the Sun [69]:

$$f_{\text{sun}}^{\text{DM}}(r, u') = \frac{1}{V_1} \left( \frac{m_\chi}{2\pi k T_\chi} \right)^{3/2} e^{-m_\chi u'^2 / (2k T_\chi)} e^{-m_\chi \phi(r) / (k T_\chi)} 2\pi u'^2 \sin \theta, \quad (3.5)$$

where  $V_1 = \int_0^{R_\odot} e^{-m_\chi \phi / (k T_\chi)} 4\pi r^2 dr$ ,  $\phi(r)$  is the solar gravitational potential, and  $T_\chi$  is the dark matter temperature in the Sun<sup>5</sup>. The effective dark matter self-scattering cross section is  $\sigma^{\text{eff}}(v_{\text{rel}}) = (\sigma_{\chi\chi}^{\text{att}} + \sigma_{\chi\chi}^{\text{rep}})/2$ , accounting for both attractive and repulsive interactions. The relative speed is  $v_{\text{rel}} = (v^2 + u^2 + u'^2 - 2u'\sqrt{v^2 + u^2} \cos \theta)^{1/2}$ , where  $\theta$  the angle between the velocity of the incoming particle and the one already captured in the Sun. Finally,  $\Theta$  is the Heaviside step function. We integrate equation(3.3) over the dark matter particles' velocities in the halo ( $u$ ) and in the Sun ( $u'$ ) and over the Sun's volume.

Figure 2 shows the total dark matter capture rate  $\Gamma_c + \Gamma_s(t_\odot)$  at the present epoch  $t = t_\odot$  for  $\varepsilon_Z = 10^{-9}$  and  $\varepsilon_\gamma = 0$ . The red dashed contours indicate the self-capture contribution relative to the total rate, while the region in between the orange dashed curves indicates the vdSIDM region that alleviates the too big to fail problem with  $0.1 < \langle \sigma_T \rangle / m_\chi < 10$  cm<sup>2</sup>/g, assuming a characteristic dwarf velocity of  $v_0 = 30$  km/s. It is clear that the dark matter self-interaction contribution to the total capture rate is negligible for most of the parameter space.

The annihilation rate  $\Gamma_a$  is given by

$$\Gamma_a = \int d^3r n_\chi(r) n_{\bar{\chi}}(r) \langle \sigma_a v \rangle, \quad (3.6)$$

where  $\langle \sigma_a v \rangle$  is the thermally averaged dark matter annihilation cross section and  $n_\chi(r)$  is the radial distribution of dark matter particles in the Sun. This equation can be rewritten as  $\Gamma_a = C_a N_\chi^2 / 4$ , where  $N_\chi$  is the total number of dark matter particles and  $C_a = \langle \sigma_a v \rangle / V_{\text{eff}}$ , with effective volume  $V_{\text{eff}} = 6.9 \times 10^{27} \left( \frac{T_\chi}{1.57 \times 10^7 \text{ K}} \right)^{3/2} \left( \frac{100 \text{ GeV}}{m_\chi} \right)^{3/2} \text{ cm}^3$  [70]. The thermally averaged cross section is

$$\langle \sigma_a v \rangle = \left( \frac{m_\chi}{4\pi k T_\chi} \right)^{3/2} \int d^3v e^{-\frac{m_\chi v^2}{4k T_\chi}} (\sigma_a v), \quad (3.7)$$

<sup>5</sup>For most  $m_\chi$  values, the dark matter temperature is equal to the Sun's core temperature  $T_\chi = 1.57 \times 10^7$  K. However for  $m_\chi \lesssim 10$  GeV a correction is needed, since in this case the particles are more dispersedly distributed around the solar core, reaching distances where the solar temperature is lower. Hence, for these lower masses, we considered  $T_\chi$  equal to the solar temperature at the dark matter mean distance from the Sun's core, e.g.  $T_\chi = 1.43 \times 10^7$  K and  $1.52 \times 10^7$  K for  $m_\chi = 4$  and 10 GeV respectively.



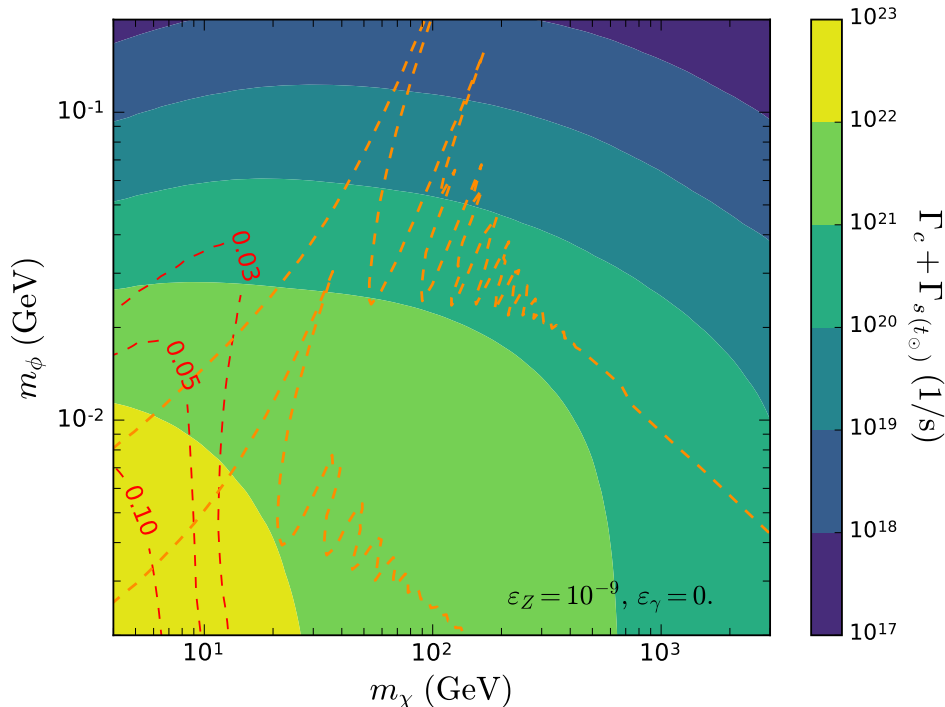


**Figure 2.** Total dark matter capture rate, where  $\varepsilon_Z = 10^{-9}$  and  $\varepsilon_\gamma = 0$ .

where  $(\sigma_a v)$  includes the Sommerfeld enhancement factor. The effect of this factor over  $C_a$  is clearly seen in figure 3, where the ratio  $C_a/C_a^{\text{w/o Sommm.}}$  of  $C_a$  including over excluding the Sommerfeld factor is shown. It can be seen that  $C_a$  is greatly enhanced by this factor, specially at large masses  $m_\chi > 100$  GeV. This is expected, since the average dark matter velocity in the Sun decreases for large  $m_\chi$ .

Once the total capture and annihilation rates are obtained, the total number of DM particles in the Sun at a age  $t$  is given by equation(3.1), which yields to

$$N_\chi(t) = \frac{\Gamma_c \tanh(t/\zeta)}{\zeta^{-1} - C_s \tanh(t/\zeta)/2}, \quad (3.8)$$

where  $\zeta = (\Gamma_c C_a/2 + C_s^2/4)^{-1/2}$  [80]. So, at present time  $t_\odot = 4.57 \times 10^9$  years, and the annihilation rate is  $\Gamma_a = C_a N_\chi^2(t_\odot)/4$ .

The time evolution of the captured dark matter particles and their corresponding annihilation rates are shown in figure 4. The solid curves represent our results for the full calculation as described above, while the dotted curves neglect the DM self-capture term, and the dashed curves ignore the Sommerfeld enhancement in DM annihilations. The effect of DM self-interactions is only noticeable when the DM–nucleon cross section is very low, which happens for  $\varepsilon_Z = 10^{-10}$  (blue curves). In this case, both the number of captured particles and the annihilation rate increase. On the other hand, the Sommerfeld enhancement in the annihilation rate hastens the equilibrium. This effect is more evident for  $\varepsilon_Z = 10^{-8}$  and  $10^{-9}$  (red and green curves). Although this lowers the total number of captured particles,

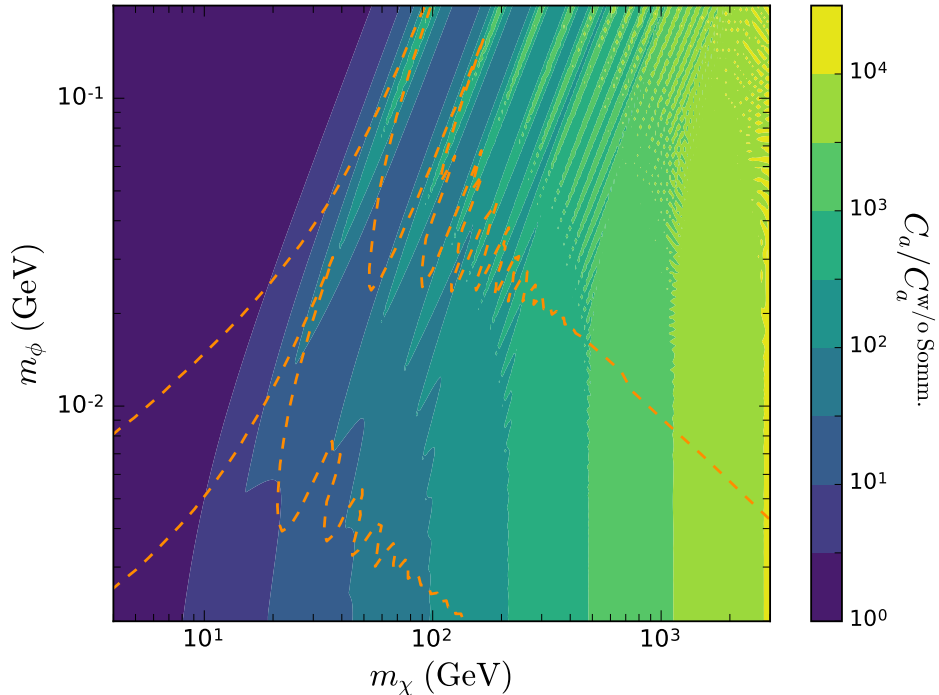


**Figure 3.** Sommerfeld enhancement effect on  $C_a$ .

the annihilation rate is much larger and reaches its maximum much earlier. However, notice that the Sommerfeld enhancement does not necessarily cause a larger annihilation rate at the present time (highlighted by the dotted vertical line), as is the case for  $\varepsilon_Z = 10^{-8}$ .

#### 4 Neutrino Signal and Background

The annihilation of dark matter particles in the Sun creates pairs of  $\phi$  particles which, through their subsequent decay, produces high energy electrons and neutrinos. In this analysis we focus on the neutrino signal, estimating its flux at Earth and both IceCube-DeepCore [82] and PINGU's [83] sensitivity to vdSIDM models. In this way, we determine the vdSIDM parameter space to be probed by these telescopes.

The neutrinos and anti-neutrinos<sup>6</sup> production is flavor blind, and their energy spectrum per annihilation is given by:

$$\frac{dN_\nu}{dE_\nu} = \frac{4}{\Delta E} \Theta(E_\nu - E_-) \Theta(E_+ - E_\nu), \quad (4.1)$$

where  $\Delta E = \sqrt{m_\chi^2 - m_\phi^2}$  with its maximum and minimum energies at  $E_\pm = (m_\chi \pm \sqrt{m_\chi^2 - m_\phi^2})/2$ , or in our case  $E_- \approx 0$  and  $E_+ \approx m_\chi$ . Neutrino production is maximum when only  $Z$  mass

<sup>6</sup>From here on when we mention neutrinos, we consider them in conjunction with anti-neutrinos, unless specified.

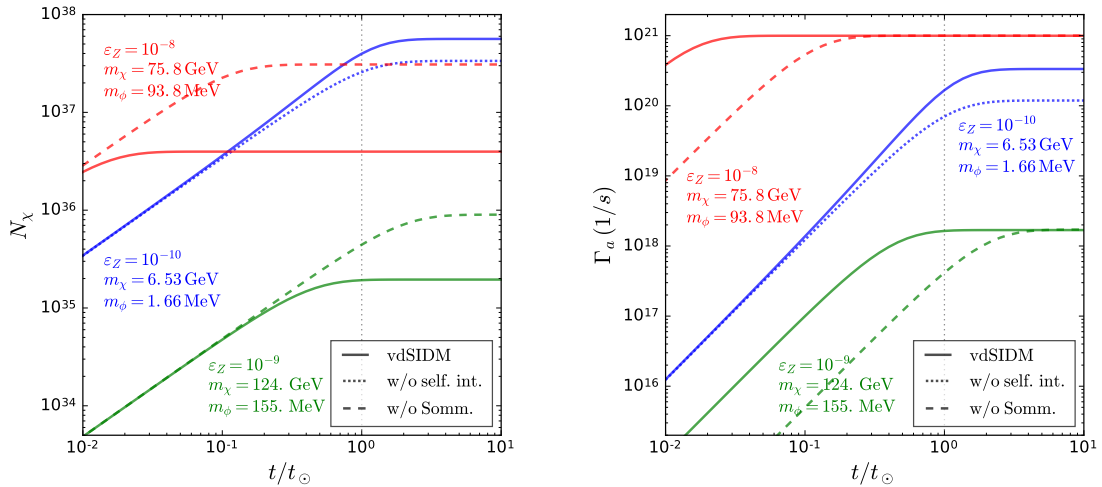


**Figure 4.** The time evolution of captured dark matter particles for three representative cases (left) and their corresponding annihilation rates (right). Solid curves represent results for the full calculation as described in the text, dotted curves neglect the DM self-capture term, dashes curves ignore the Sommerfeld enhancement in DM annihilations.

mixing is considered, or in other words, when  $\varepsilon_\gamma = 0$ . Here we consider this scenario, for which  $BR(\phi \rightarrow \nu\bar{\nu}) \approx 86\%$ . We also consider additional cases, where  $\varepsilon_\gamma = -0.64 \times \varepsilon_Z$ , such that the  $\phi$  couplings to protons and neutrons are equal ( $\eta \equiv \varepsilon_n/\varepsilon_p = 1$ ), with  $BR(\phi \rightarrow \nu\bar{\nu}) \approx 74\%$ , and  $\eta = -0.7$  with a 68% branching ratio.

It is important to note that the neutrinos are not necessarily produced at the Sun’s core, since the  $\phi$  mediators propagate freely until their decay.<sup>7</sup> Thus, the neutrino production point depends strongly on the mixing parameters as well as on the  $\phi$ ’s Lorentz factor. For example, for pure  $Z$  mixing, the mean decay length in the Sun is given by

$$\lambda_\phi \approx 4 \times 10^{-2} R_\odot \times \left( \frac{10^{-8}}{\varepsilon_Z} \right)^2 \left( \frac{10 \text{ MeV}}{m_\phi} \right) \left( \frac{m_\chi/m_\phi}{1000} \right) \quad (4.2)$$

The  $\phi$  decay probability distribution is shown in figure 5 for two cases:  $\varepsilon_Z = 10^{-8}$ ,  $m_\phi = 10 \text{ MeV}$ ,  $m_\chi = 10 \text{ GeV}$  (blue) and  $m_\chi = 1 \text{ TeV}$  (red). In the blue distribution most ( $\sim 67\%$ ) of the  $\phi$  mediators decay within the inner part of the Sun ( $r \leq R_\odot/2$ ), while for the red distribution, due to the larger Lorentz boost, most decays ( $\sim 81\%$ ) occur outside the Sun.

To determine the neutrino flux at the detector, we developed a simulation code where the neutrino point of production is selected accordingly to the  $\phi$  decay distribution. For each combination of parameters ( $\varepsilon_\gamma, \varepsilon_Z, m_\chi, m_\phi$ ) we considered  $5 \times 10^5$  annihilation events. Neutrinos were propagated to the detector [84–87] taking into account neutral and charged current interactions, oscillations and the production of secondary neutrinos. We used the density profile of the Sun as given by the standard solar model BS05OP [76]. Propagation from the Sun’s surface to a distance of 1 AU (Earth’s approximate average distance from the Sun), included neutrinos produced in this region, as well as oscillations in the vacuum.

<sup>7</sup>Due to the very small mixing parameters  $\varepsilon_\gamma, \varepsilon_Z$ , the  $\phi$  mediator–nucleon cross section is also very small, being  $\sigma_{\phi p} \sim 10^{-46} \text{ cm}^2$ , which implies that their interaction length is much greater than the Sun radius.

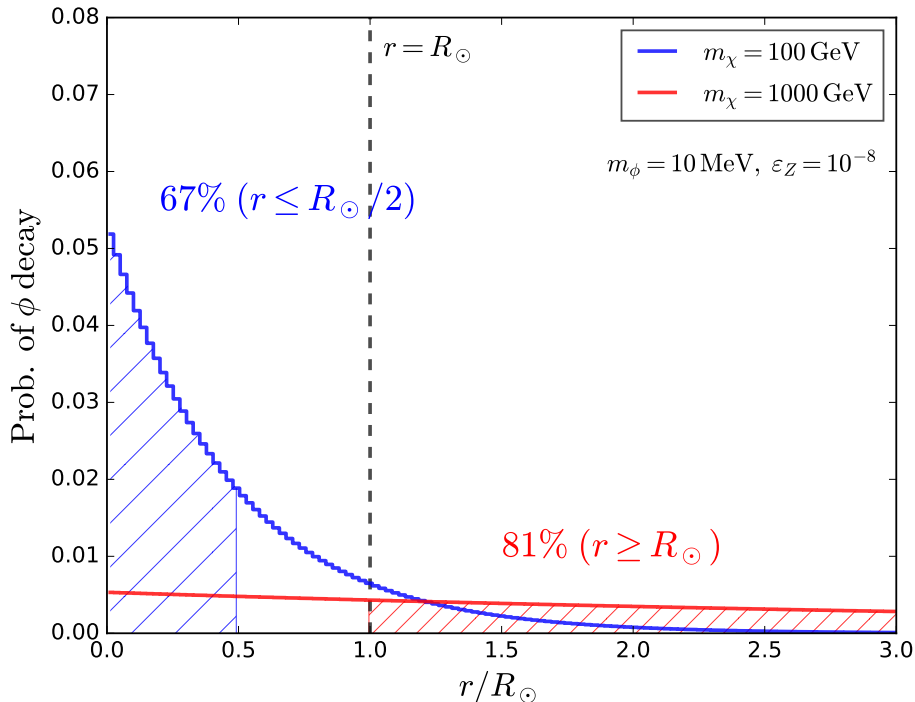


**Figure 5.**  $\phi$  mediator decay probability as a function of the distance from the Sun’s core. For 100 GeV dark matter, most decays (67%) occur inside the Sun with  $r \leq R_\odot/2$ , while for 1 TeV, most decays (81%) occur outside the Sun.

Finally, they were propagated from 1 AU to the detectors’s location at the Earth considering their observational time. For this latter step we used the WimpEvent program, contained in the WimpSim simulation package [86].<sup>8</sup>

The number of neutrino signal events  $N_\nu^s$  in the detector is given by

$$N_\nu^s = \Gamma_a t_{\text{exp}} \times \int_{\Delta\Omega} \int_{E_{\text{th}}}^{m_\chi} \frac{d^2\phi_\nu}{dE_\nu d\Omega} A_{\text{eff}}(E_\nu) dE_\nu d\Omega \quad (4.3)$$

where  $t_{\text{exp}}$  is the detector’s exposure time,  $\phi_\nu$  is the neutrino flux at the detector per annihilation,  $E_{\text{th}}$  is the detector energy threshold and the maximum neutrino energy is  $m_\chi$ .  $A_{\text{eff}}(E_\nu)$  is the detector’s effective area as a function of the neutrino energy  $E_\nu$  [89, 90]. The latter accounts for the neutrino-nucleon interaction probability and the produced muon energy loss before detection, as well as for the detector’s trigger and selection analysis efficiencies.

To estimate the number of signal events we took into account the detector’s angular resolution. The neutrino arrival direction was smeared following a gaussian distribution with its standard deviation given by the detector’s angular resolution [83, 89] at the corresponding neutrino energy. Only events arriving within a solid angle  $\Delta\Omega = 2\pi(1 - \cos\Psi)$  surrounding

<sup>8</sup>For consistency we used WimpSim 3.05 default values for the neutrino oscillation parameters, as well as the neutrino–nucleon cross sections (calculated with CTEQ6-DIS PDFs [88]).

the direction between the detector and the Sun were accepted. The acceptance angle  $\Psi$  depends on energy and specific analysis, and will be defined in the next section.

Muons and neutrinos produced by cosmic rays' interactions in the Earth's atmosphere constitutes the main background in our analysis. As the IceCube collaboration achieves an excellent atmospheric muon rejection [89], we consider that the background is comprised exclusively by the irreducible flux of atmospheric neutrinos.

The number of background events is given by

$$N_\nu^b = t_{\text{exp}} \times \int_{E_{\text{th}}}^{E_{\text{max}}} \frac{d\phi_{\nu_{\text{atm}}}}{dE_\nu} A_\nu(E_\nu) dE_\nu \times \Delta\Omega \quad (4.4)$$

where  $\phi_{\nu_{\text{atm}}}$  is the atmospheric neutrino flux at the detector's location [91].

## 5 IceCube-DeepCore and PINGU Sensitivity to vdSIDM

The IceCube neutrino telescope has a good sensitivity for neutrinos arriving from the Sun's direction, and thanks to its more recent inner array DeepCore, can lower its energy threshold to about  $\sim 10$  GeV [82]. It also has a good angular resolution for muon neutrinos, ranging from  $\sim 5^\circ$  at 100 GeV to  $\sim 1^\circ$  at 1 TeV [89].

In order to determine the IceCube-DeepCore sensitivity to vdSIDM, we considered the same time period as the latest IceCube collaboration's search for dark matter annihilating in the Sun [89]. It spanned a three year period including the austral winters between May 2011 and May 2014, with a total lifetime exposure of  $t_{\text{exp}} = 532$  days. To be compatible with their procedure, we only considered up-going muon neutrinos. We split the results of our simulations into three samples: events with  $m_\chi \leq 50$  GeV, for which dark matter annihilations result mainly in low energies neutrinos, and therefore can only be detected by DeepCore; events with  $m_\chi \geq 500$  GeV, for which we considered the full IceCube's effective area, and finally events with intermediate masses where we performed a combined analysis. Accordingly, we take the acceptance angles  $\Psi_1 = 10^\circ$  and  $\Psi_2 = 2.8^\circ$  as reference values, where the first corresponds to DeepCore's angular cut, as defined in their analysis, and the second to the their first angular bin [89]. This latter value allows us to take advantage of the better angular resolution at higher energies.

The number of background events was determined by the average atmospheric muon neutrino flux from the Sun's direction in the winter [91]. Since during this season the Sun's zenith angle varies between  $90^\circ$  and  $113.5^\circ$  we took only the average within these directions.

Additionally, we determined the planned IceCube's extension PINGU [83] sensitivity to vdSIDM. PINGU consists of 40 new strings with 60 optical modules each in the DeepCore region of the IceCube detector, lowering the energy threshold to just a few GeV. As a consequence, vdSIDM can be probed to lower masses, more specifically between 4 and 30 GeV. The same procedure as for the IceCube-DeepCore analysis was followed for the the PINGU detector, for which we used the angular resolution given in [83] and the effective area in [90].

Our results are shown in figures 6 and 7, each for different values of the mixing parameter  $\varepsilon_Z$ . The regions below or enclosed by the colored curves correspond to  $(m_\chi, m_\phi)$  values for which IceCube-DeepCore and PINGU detectors have at least a 2-sigma detection sensitivity relative to the expected background of atmospheric muon neutrinos. The solid curves are for an acceptance angle  $\Psi_1 = 10^\circ$  while dashed curves are for  $\Psi_2 = 2.8^\circ$ . Each color correspond to different  $\varepsilon_\gamma$  or  $\eta \equiv \varepsilon_n/\varepsilon_p$  value, as labeled. The discontinuity of the curves around  $m_\chi = 30$  GeV reflects the two individual analysis, one for the IceCube-DeepCore and the

other for the PINGU detector. The region between the orange dashed curves correspond to the vdSIDM parameter space that alleviates the too big to fail problem, having  $0.1 < \langle \sigma_T \rangle / m_\chi < 10 \text{ cm}^2/\text{g}$ . For  $\varepsilon_Z = 10^{-8}$ , this parameter space can be almost completely probed by these experiments, while for  $\varepsilon_Z = 10^{-9}$  a large part of this region can be probed.

For comparison we derive direct detection limits from the LUX experiment recent results [92]. We followed the procedure described in [29], considering the  $q^2$ -dependent suppression factor given by equation (2.13) and taking  $q \approx 50 \text{ MeV}$  for dark matter - xenon scattering. Additionally, we determined the limits in the case of isospin violation with  $\eta = -0.7$  [93]. These limits are represented by the red dotted curves in the figures described above, where the region below them are excluded at 90% C.L. Notice that figure 7 does not include the direct detection limit for  $\eta = -0.7$  since it falls out of the explored parameter space, which indicates the high dependence of direct detection results on the isospin violation parameter in contrast to that of the neutrino telescopes.

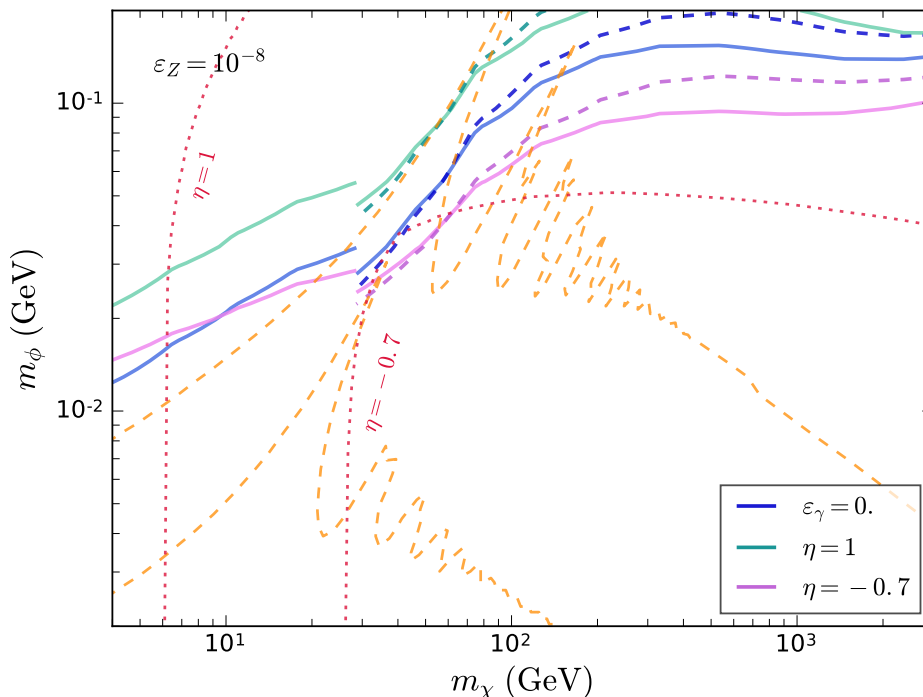


**Figure 6.** Sensitivity of IceCube-DeepCore and PINGU for vdSIDM for  $\varepsilon_Z = 10^{-8}$ , where the region below the curves (as labeled) can be probed by these experiments. The region between the orange dashed curves correspond to the vdSIDM parameter space that alleviates the too big to fail problem, having  $0.1 < \langle \sigma_T \rangle / m_\chi < 10 \text{ cm}^2/\text{g}$ . The red dotted curves correspond to limits derived from direct detection (LUX) results, see text for more details.

## 6 Conclusions

We have explored vdSIDM models that can alleviate the small scale structure problems observed in dwarf galaxies. We determined neutrino telescopes sensitivity to these models,

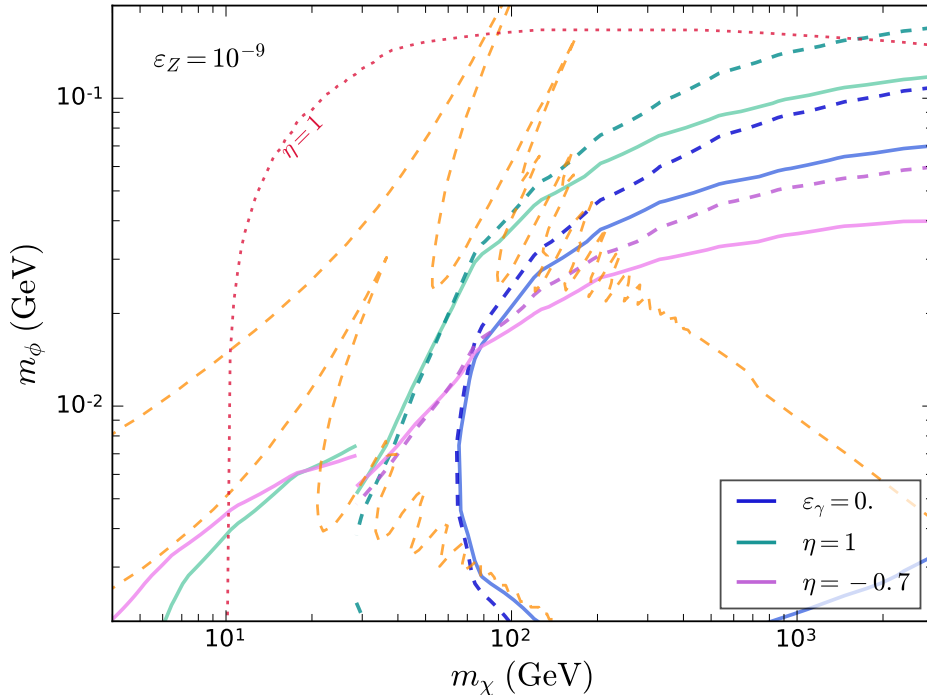


**Figure 7.** Same as figure 6, but now for  $\varepsilon_Z = 10^{-9}$ .

assuming plausible values for its parameters. Our main results are shown in figures 6 and 7.

We conclude that, for  $\varepsilon_Z = 10^{-8}$  the detector’s sensitivity is enough to probe the vast majority of the relevant vdSIDM parameter space for all  $\varepsilon_\gamma$  analyzed values, including the low dark matter mass region, thanks to the PINGU detector. These results show that neutrino telescopes can compete and complement the results from dark matter direct detection searches.

Although the sensitivity decreases for  $\varepsilon_Z = 10^{-9}$  it is still enough to probe most of the parameter space for  $m_\chi \gtrsim 70$  GeV. In this case the PINGU detector has almost no sensitivity for vdSIDM models. Also, IceCube’s sensitivity for low  $m_\phi$  and high  $m_\chi$  has a lower limit, as evidenced by the blue line at the lower right corner of figure 7. This results from the  $\phi$ ’s decay length which, in this region, is larger than the Earth–Sun’s distance, and therefore fewer neutrinos are produced. Finally, neutrino telescopes lose all sensitivity for  $\varepsilon_Z \leq 10^{-10}$ .

We have shown that the IceCube-DeepCore neutrino telescope with its current accumulated data is sensitive to most of the parameter space of vdSIDM models that alleviate the small scale structure problems observed in dwarf galaxies. Experimental analysis could probe these models, and independently confirm direct detection limits. It can also expand these limits, specially in the case of isospin violation, where we have shown that IceCube-DeepCore sensitivity is drastically better than direct detection.

## Acknowledgments

IA acknowledges the support of the São Paulo Research Foundation (FAPESP), grant (2016/09084-0). IA also acknowledges the partial support from the Brazilian National Council for Scientific Research (CNPq). DSR was funded by FAPESP. This project has received funding from the European Unions Horizon 2020 research and innovative programme under Marie Skłodowska-Curie grant agreement No 674896.

## References

- [1] D. H. Weinberg, J. S. Bullock, F. Governato, R. Kuzio de Naray and A. H. G. Peter, *Cold dark matter: controversies on small scales*, *Proc. Nat. Acad. Sci.* **112** (2014) 12249–12255, [[1306.0913](#)].
- [2] A. Del Popolo and M. Le Delliou, *Small scale problems of the  $\Lambda$ CDM model: a short review*, *Galaxies* **5** (2017) 17, [[1606.07790](#)].
- [3] W. J. G. de Blok, *The Core-Cusp Problem*, *Adv. Astron.* **2010** (2010) 789293, [[0910.3538](#)].
- [4] S.-H. Oh, W. J. G. de Blok, E. Brinks, F. Walter and R. C. Kennicutt, Jr, *Dark and luminous matter in THINGS dwarf galaxies*, *Astron. J.* **141** (2011) 193, [[1011.0899](#)].
- [5] R. Kuzio de Naray, S. S. McGaugh and W. J. G. de Blok, *Mass Models for Low Surface Brightness Galaxies with High Resolution Optical Velocity Fields*, *Astrophys. J.* **676** (2008) 920–943, [[0712.0860](#)].
- [6] J. F. Navarro, C. S. Frenk and S. D. M. White, *A Universal density profile from hierarchical clustering*, *Astrophys. J.* **490** (1997) 493–508, [[astro-ph/9611107](#)].
- [7] J. F. Navarro, A. Ludlow, V. Springel, J. Wang, M. Vogelsberger, S. D. M. White et al., *The Diversity and Similarity of Cold Dark Matter Halos*, *Mon. Not. Roy. Astron. Soc.* **402** (2010) 21, [[0810.1522](#)].
- [8] J. Stadel, D. Potter, B. Moore, J. Diemand, P. Madau, M. Zemp et al., *Quantifying the heart of darkness with GALO - a multi-billion particle simulation of our galactic halo*, *Mon. Not. Roy. Astron. Soc.* **398** (2009) L21–L25, [[0808.2981](#)].
- [9] M. Boylan-Kolchin, J. S. Bullock and M. Kaplinghat, *Too big to fail? The puzzling darkness of massive Milky Way subhaloes*, *Mon. Not. Roy. Astron. Soc.* **415** (2011) L40, [[1103.0007](#)].
- [10] M. Boylan-Kolchin, J. S. Bullock and M. Kaplinghat, *The Milky Way’s bright satellites as an apparent failure of LCDM*, *Mon. Not. Roy. Astron. Soc.* **422** (2012) 1203–1218, [[1111.2048](#)].
- [11] D. N. Spergel and P. J. Steinhardt, *Observational evidence for selfinteracting cold dark matter*, *Phys. Rev. Lett.* **84** (2000) 3760–3763, [[astro-ph/9909386](#)].
- [12] A. Burkert, *The Structure and evolution of weakly selfinteracting cold dark matter halos*, *Astrophys. J.* **534** (2000) L143–L146, [[astro-ph/0002409](#)].
- [13] B. Moore, S. Gelato, A. Jenkins, F. R. Pearce and V. Quilis, *Collisional versus collisionless dark matter*, *Astrophys. J.* **535** (2000) L21–L24, [[astro-ph/0002308](#)].
- [14] R. Dave, D. N. Spergel, P. J. Steinhardt and B. D. Wandelt, *Halo properties in cosmological simulations of selfinteracting cold dark matter*, *Astrophys. J.* **547** (2001) 574–589, [[astro-ph/0006218](#)].
- [15] M. Vogelsberger, J. Zavala and A. Loeb, *Subhaloes in Self-Interacting Galactic Dark Matter Haloes*, *Mon. Not. Roy. Astron. Soc.* **423** (2012) 3740, [[1201.5892](#)].
- [16] J. Zavala, M. Vogelsberger and M. G. Walker, *Constraining Self-Interacting Dark Matter with the Milky Way’s dwarf spheroidals*, *Mon. Not. Roy. Astron. Soc.* **431** (2013) L20–L24, [[1211.6426](#)].



- [17] O. D. Elbert, J. S. Bullock, S. Garrison-Kimmel, M. Rocha, J. Oñorbe and A. H. G. Peter, *Core formation in dwarf haloes with self-interacting dark matter: no fine-tuning necessary*, *Mon. Not. Roy. Astron. Soc.* **453** (2015) 29–37, [[1412.1477](#)].
- [18] S. W. Randall, M. Markevitch, D. Clowe, A. H. Gonzalez and M. Bradac, *Constraints on the Self-Interaction Cross-Section of Dark Matter from Numerical Simulations of the Merging Galaxy Cluster 1E 0657-56*, *Astrophys. J.* **679** (2008) 1173–1180, [[0704.0261](#)].
- [19] A. Robertson, R. Massey and V. Eke, *What does the Bullet Cluster tell us about self-interacting dark matter?*, *Mon. Not. Roy. Astron. Soc.* **465** (2017) 569–587, [[1605.04307](#)].
- [20] D. Harvey, R. Massey, T. Kitching, A. Taylor and E. Tittley, *The non-gravitational interactions of dark matter in colliding galaxy clusters*, *Science* **347** (2015) 1462–1465, [[1503.07675](#)].
- [21] I. F. M. Albuquerque, C. Pérez de Los Heros and D. S. Robertson, *Constraints on self interacting dark matter from IceCube results*, *JCAP* **1402** (2014) 047, [[1312.0797](#)].
- [22] M. Rocha, A. H. G. Peter, J. S. Bullock, M. Kaplinghat, S. Garrison-Kimmel, J. Onorbe et al., *Cosmological Simulations with Self-Interacting Dark Matter I: Constant Density Cores and Substructure*, *Mon. Not. Roy. Astron. Soc.* **430** (2013) 81–104, [[1208.3025](#)].
- [23] A. H. G. Peter, M. Rocha, J. S. Bullock and M. Kaplinghat, *Cosmological Simulations with Self-Interacting Dark Matter II: Halo Shapes vs. Observations*, *Mon. Not. Roy. Astron. Soc.* **430** (2013) 105, [[1208.3026](#)].
- [24] J. L. Feng, M. Kaplinghat and H.-B. Yu, *Halo Shape and Relic Density Exclusions of Sommerfeld-Enhanced Dark Matter Explanations of Cosmic Ray Excesses*, *Phys. Rev. Lett.* **104** (2010) 151301, [[0911.0422](#)].
- [25] A. Loeb and N. Weiner, *Cores in Dwarf Galaxies from Dark Matter with a Yukawa Potential*, *Phys. Rev. Lett.* **106** (2011) 171302, [[1011.6374](#)].
- [26] S. Tulin, H.-B. Yu and K. M. Zurek, *Beyond Collisionless Dark Matter: Particle Physics Dynamics for Dark Matter Halo Structure*, *Phys. Rev.* **D87** (2013) 115007, [[1302.3898](#)].
- [27] N. Arkani-Hamed, D. P. Finkbeiner, T. R. Slatyer and N. Weiner, *A Theory of Dark Matter*, *Phys. Rev.* **D79** (2009) 015014, [[0810.0713](#)].
- [28] J. L. Feng, M. Kaplinghat and H.-B. Yu, *Sommerfeld Enhancements for Thermal Relic Dark Matter*, *Phys. Rev.* **D82** (2010) 083525, [[1005.4678](#)].
- [29] M. Kaplinghat, S. Tulin and H.-B. Yu, *Direct Detection Portals for Self-interacting Dark Matter*, *Phys. Rev.* **D89** (2014) 035009, [[1310.7945](#)].
- [30] E. Del Nobile, M. Kaplinghat and H.-B. Yu, *Direct Detection Signatures of Self-Interacting Dark Matter with a Light Mediator*, *JCAP* **1510** (2015) 055, [[1507.04007](#)].
- [31] T. Bringmann, F. Kahlhoefer, K. Schmidt-Hoberg and P. Walia, *Strong constraints on self-interacting dark matter with light mediators*, *Phys. Rev. Lett.* **118** (2017) 141802, [[1612.00845](#)].
- [32] M. Cirelli, P. Panci, K. Petraki, F. Sala and M. Taoso, *Dark Matter’s secret liaisons: phenomenology of a dark  $U(1)$  sector with bound states*, *JCAP* **1705** (2017) 036, [[1612.07295](#)].
- [33] N. F. Bell and K. Petraki, *Enhanced neutrino signals from dark matter annihilation in the Sun via metastable mediators*, *JCAP* **1104** (2011) 003, [[1102.2958](#)].
- [34] J. L. Feng, J. Smolinsky and P. Tanedo, *Detecting dark matter through dark photons from the Sun: Charged particle signatures*, *Phys. Rev.* **D93** (2016) 115036, [[1602.01465](#)].
- [35] R. K. Leane, K. C. Y. Ng and J. F. Beacom, *Powerful Solar Signatures of Long-Lived Dark Mediators*, *Phys. Rev.* **D95** (2017) 123016, [[1703.04629](#)].
- [36] M. R. Buckley and P. J. Fox, *Dark Matter Self-Interactions and Light Force Carriers*, *Phys. Rev.* **D81** (2010) 083522, [[0911.3898](#)].

- [37] L. G. van den Aarssen, T. Bringmann and C. Pfrommer, *Is dark matter with long-range interactions a solution to all small-scale problems of  $\Lambda$ CDM cosmology?*, *Phys. Rev. Lett.* **109** (2012) 231301, [[1205.5809](#)].
- [38] A. Sommerfeld, *Über die Beugung und Bremsung der Elektronen*, *Ann. der Physik* **403** (1931) 257.
- [39] J. Hisano, S. Matsumoto, M. M. Nojiri and O. Saito, *Non-perturbative effect on dark matter annihilation and gamma ray signature from galactic center*, *Phys. Rev.* **D71** (2005) 063528, [[hep-ph/0412403](#)].
- [40] S. Cassel, *Sommerfeld factor for arbitrary partial wave processes*, *J. Phys.* **G37** (2010) 105009, [[0903.5307](#)].
- [41] T. R. Slatyer, *The Sommerfeld enhancement for dark matter with an excited state*, *JCAP* **1002** (2010) 028, [[0910.5713](#)].
- [42] H. Davoudiasl, H.-S. Lee and W. J. Marciano, *'Dark' Z implications for Parity Violation, Rare Meson Decays, and Higgs Physics*, *Phys. Rev.* **D85** (2012) 115019, [[1203.2947](#)].
- [43] B. Holdom, *Two  $U(1)$ 's and Epsilon Charge Shifts*, *Phys. Lett.* **166B** (1986) 196–198.
- [44] M. Pospelov and A. Ritz, *Astrophysical Signatures of Secluded Dark Matter*, *Phys. Lett.* **B671** (2009) 391–397, [[0810.1502](#)].
- [45] J. D. Bjorken, R. Essig, P. Schuster and N. Toro, *New Fixed-Target Experiments to Search for Dark Gauge Forces*, *Phys. Rev.* **D80** (2009) 075018, [[0906.0580](#)].
- [46] R. Foot and S. Vagnozzi, *Dissipative hidden sector dark matter*, *Phys. Rev.* **D91** (2015) 023512, [[1409.7174](#)].
- [47] K. S. Babu, C. F. Kolda and J. March-Russell, *Implications of generalized Z - Z-prime mixing*, *Phys. Rev.* **D57** (1998) 6788–6792, [[hep-ph/9710441](#)].
- [48] Y. Cui and F. D'Eramo, *On the Completeness of Vector Portal Theories: New Insights into the Dark Sector and its Interplay with Higgs Physics*, 2017.
- [49] P. Langacker, *The Physics of Heavy  $Z'$  Gauge Bosons*, *Rev. Mod. Phys.* **81** (2009) 1199–1228, [[0801.1345](#)].
- [50] R. Foot, *Mirror dark matter and the new DAMA/LIBRA results: A Simple explanation for a beautiful experiment*, *Phys. Rev.* **D78** (2008) 043529, [[0804.4518](#)].
- [51] N. Fornengo, P. Panci and M. Regis, *Long-Range Forces in Direct Dark Matter Searches*, *Phys. Rev.* **D84** (2011) 115002, [[1108.4661](#)].
- [52] T. Lin, H.-B. Yu and K. M. Zurek, *On Symmetric and Asymmetric Light Dark Matter*, *Phys. Rev.* **D85** (2012) 063503, [[1111.0293](#)].
- [53] J. B. Dent, F. Ferrer and L. M. Krauss, *Constraints on Light Hidden Sector Gauge Bosons from Supernova Cooling*, 2012.
- [54] H. K. Dreiner, J.-F. Fortin, C. Hanhart and L. Ubaldi, *Supernova constraints on MeV dark sectors from  $e^+e^-$  annihilations*, *Phys. Rev.* **D89** (2014) 105015, [[1310.3826](#)].
- [55] D. Kazanas, R. N. Mohapatra, S. Nussinov, V. L. Teplitz and Y. Zhang, *Supernova Bounds on the Dark Photon Using its Electromagnetic Decay*, *Nucl. Phys.* **B890** (2014) 17–29, [[1410.0221](#)].
- [56] E. Rrapaj and S. Reddy, *Nucleon-nucleon bremsstrahlung of dark gauge bosons and revised supernova constraints*, *Phys. Rev.* **C94** (2016) 045805, [[1511.09136](#)].
- [57] E. Hardy and R. Lasenby, *Stellar cooling bounds on new light particles: plasma mixing effects*, *JHEP* **02** (2017) 033, [[1611.05852](#)].

- [58] J. H. Chang, R. Essig and S. D. McDermott, *Revisiting Supernova 1987A Constraints on Dark Photons*, *JHEP* **01** (2017) 107, [[1611.03864](#)].
- [59] J. D. Bjorken, S. Ecklund, W. R. Nelson, A. Abashian, C. Church, B. Lu et al., *Search for Neutral Metastable Penetrating Particles Produced in the SLAC Beam Dump*, *Phys. Rev.* **D38** (1988) 3375.
- [60] B. Batell, M. Pospelov and A. Ritz, *Exploring Portals to a Hidden Sector Through Fixed Targets*, *Phys. Rev.* **D80** (2009) 095024, [[0906.5614](#)].
- [61] R. Essig, R. Harnik, J. Kaplan and N. Toro, *Discovering New Light States at Neutrino Experiments*, *Phys. Rev.* **D82** (2010) 113008, [[1008.0636](#)].
- [62] CHARM collaboration, F. Bergsma et al., *A Search for Decays of Heavy Neutrinos in the Mass Range 0.5-GeV to 2.8-GeV*, *Phys. Lett.* **166B** (1986) 473–478.
- [63] S. N. Gninenko, *Constraints on sub-GeV hidden sector gauge bosons from a search for heavy neutrino decays*, *Phys. Lett.* **B713** (2012) 244–248, [[1204.3583](#)].
- [64] FERMI-LAT collaboration, M. Ackermann et al., *Searching for Dark Matter Annihilation from Milky Way Dwarf Spheroidal Galaxies with Six Years of Fermi Large Area Telescope Data*, *Phys. Rev. Lett.* **115** (2015) 231301, [[1503.02641](#)].
- [65] AMS collaboration, L. Accardo et al., *High Statistics Measurement of the Positron Fraction in Primary Cosmic Rays of 0.5–500 GeV with the Alpha Magnetic Spectrometer on the International Space Station*, *Phys. Rev. Lett.* **113** (2014) 121101.
- [66] AMS collaboration, M. Aguilar et al., *Electron and Positron Fluxes in Primary Cosmic Rays Measured with the Alpha Magnetic Spectrometer on the International Space Station*, *Phys. Rev. Lett.* **113** (2014) 121102.
- [67] AMS collaboration, M. Aguilar et al., *Antiproton Flux, Antiproton-to-Proton Flux Ratio, and Properties of Elementary Particle Fluxes in Primary Cosmic Rays Measured with the Alpha Magnetic Spectrometer on the International Space Station*, *Phys. Rev. Lett.* **117** (2016) 091103.
- [68] PLANCK collaboration, P. A. R. Ade et al., *Planck 2015 results. XIII. Cosmological parameters*, *Astron. Astrophys.* **594** (2016) A13, [[1502.01589](#)].
- [69] A. Gould, *WIMP Distribution in and Evaporation From the Sun*, *Astrophys. J.* **321** (1987) 560.
- [70] K. Griest and D. Seckel, *Cosmic Asymmetry, Neutrinos and the Sun*, *Nucl. Phys.* **B283** (1987) 681–705.
- [71] B. von Harling and K. Petraki, *Bound-state formation for thermal relic dark matter and unitarity*, *JCAP* **1412** (2014) 033, [[1407.7874](#)].
- [72] P. Salucci, F. Nesti, G. Gentile and C. F. Martins, *The dark matter density at the Sun’s location*, *Astron. Astrophys.* **523** (2010) A83, [[1003.3101](#)].
- [73] R. Catena and P. Ullio, *A novel determination of the local dark matter density*, *JCAP* **1008** (2010) 004, [[0907.0018](#)].
- [74] G. Jungman, M. Kamionkowski and K. Griest, *Supersymmetric dark matter*, *Phys. Rept.* **267** (1996) 195–373, [[hep-ph/9506380](#)].
- [75] M. Asplund, N. Grevesse, A. J. Sauval and P. Scott, *The chemical composition of the Sun*, *Ann. Rev. Astron. Astrophys.* **47** (2009) 481–522, [[0909.0948](#)].
- [76] J. N. Bahcall, A. M. Serenelli and S. Basu, *New solar opacities, abundances, helioseismology, and neutrino fluxes*, *Astrophys. J.* **621** (2005) L85–L88, [[astro-ph/0412440](#)].
- [77] W. H. Press and D. N. Spergel, *Capture by the sun of a galactic population of weakly interacting massive particles*, *Astrophys. J.* **296** (1985) 679–684.

- [78] A. Gould, *Resonant Enhancements in WIMP Capture by the Earth*, *Astrophys. J.* **321** (1987) 571.
- [79] A. Gould, *Cosmological density of WIMPs from solar and terrestrial annihilations*, *Astrophys. J.* **388** (1992) 338–344.
- [80] A. R. Zentner, *High-Energy Neutrinos From Dark Matter Particle Self-Capture Within the Sun*, *Phys. Rev.* **D80** (2009) 063501, [[0907.3448](#)].
- [81] R. Catena and A. Widmark, *WIMP capture by the Sun in the effective theory of dark matter self-interactions*, *JCAP* **1612** (2016) 016, [[1609.04825](#)].
- [82] ICECUBE collaboration, R. Abbasi et al., *The Design and Performance of IceCube DeepCore*, *Astropart. Phys.* **35** (2012) 615–624, [[1109.6096](#)].
- [83] ICECUBE PINGU collaboration, M. G. Aartsen et al., *Letter of Intent: The Precision IceCube Next Generation Upgrade (PINGU)*, 2014.
- [84] V. Barger, W.-Y. Keung, G. Shaughnessy and A. Tregre, *High energy neutrinos from neutralino annihilations in the Sun*, *Phys. Rev.* **D76** (2007) 095008, [[0708.1325](#)].
- [85] M. Cirelli, N. Fornengo, T. Montaruli, I. A. Sokalski, A. Strumia and F. Vissani, *Spectra of neutrinos from dark matter annihilations*, *Nucl. Phys.* **B727** (2005) 99–138, [[hep-ph/0506298](#)].
- [86] M. Blennow, J. Edsjo and T. Ohlsson, *Neutrinos from WIMP annihilations using a full three-flavor Monte Carlo*, *JCAP* **0801** (2008) 021, [[0709.3898](#)].
- [87] T. Ohlsson and H. Snellman, *Neutrino oscillations with three flavors in matter of varying density*, *Eur. Phys. J.* **C20** (2001) 507–515, [[hep-ph/0103252](#)].
- [88] J. Pumplin, D. R. Stump, J. Huston, H. L. Lai, P. M. Nadolsky and W. K. Tung, *New generation of parton distributions with uncertainties from global QCD analysis*, *JHEP* **07** (2002) 012, [[hep-ph/0201195](#)].
- [89] ICECUBE collaboration, M. G. Aartsen et al., *Search for annihilating dark matter in the Sun with 3 years of IceCube data*, *Eur. Phys. J.* **C77** (2017) 146, [[1612.05949](#)].
- [90] ICECUBE-GEN2 collaboration, K. Clark, *Status of the PINGU detector*, *PoS ICRC2015* (2016) 1174.
- [91] M. Honda, M. Sajjad Athar, T. Kajita, K. Kasahara and S. Midorikawa, *Atmospheric neutrino flux calculation using the NRLMSISE-00 atmospheric model*, *Phys. Rev.* **D92** (2015) 023004, [[1502.03916](#)].
- [92] LUX collaboration, D. S. Akerib et al., *Results from a search for dark matter in the complete LUX exposure*, *Phys. Rev. Lett.* **118** (2017) 021303, [[1608.07648](#)].
- [93] J. L. Feng, J. Kumar, D. Marfatia and D. Sanford, *Isospin-Violating Dark Matter*, *Phys. Lett.* **B703** (2011) 124–127, [[1102.4331](#)].